Thermally Assisted Tunneling of the B-H Complex in Silicon

José C. Noya, Carlos P. Herrero, and Rafael Ramírez
Instituto de Ciencia de Materiales, Consejo Superior de Investigaciones Científicas (C.S.I.C.), Campus Cantoblanco, 28049 Madrid, Spain
(Received 12 March 1997)

Jump rate constants of atomic hydrogen and deuterium in boron-doped crystalline silicon are calculated using quantum transition-state theory, based on the path-integral centroid formalism. A break in the slope of the Arrhenius plot for the jump rate of hydrogen is obtained at $T \sim 60$ K, indicating a crossover from thermally activated quasiclassical motion over a barrier to thermally assisted quantum tunneling, in good agreement with previous experimental results. For deuterium, no deviation from an Arrhenius law is found down to 30 K. It is shown that the defect complex undergoing quantum tunneling consists of hydrogen, boron, and the nearest silicon atoms. [S0031-9007(97)03525-4]

PACS numbers: 66.35.+a, 05.30.–d, 61.72.Bb

One of the most challenging problems concerning the presence of atomic hydrogen as an impurity in solids has been the nature of the diffusion process of this light atom [1,2]. Thus, for hydrogen in metals, there has been observed a crossover temperature from quasiclassical (high temperature) to quantum (low temperature) diffusion [3,4]. In crystalline semiconductors, there has been evidence for quantum tunneling of hydrogen (proton) in H-related defects in Ge [5] and Si [6]. In the last several years, the B-H complex in Si has become a prototypical model to study the interactions between hydrogen and substitutional acceptors in group-IV semiconductors. The structure of this complex is now well known: hydrogen breaks a B-Si bond and is located on the so-called bond-minimum (BM) site between the nearest B and Si atoms, which relax backwards [7–10], thus forming a Si-H bond stronger than the B-H bond. An important feature of this defect is the large amount of elastic energy associated with the lattice distorsion around the impurity. On this basis, one could argue that the large energy associated with self-trapping of H precludes quantum tunneling from one BM site to another BM site around the boron atom. However, as suggested by Stoneham [11], lattice vibrations can yield the *coincidence geometry* necessary for impurity jumps via tunneling. In this line, Cheng and Stavola [12], by combining stress-induced dichroism results at low temperature ($50 < T < 70$ K) [13] with previous internal friction experiments at higher temperatures ($T > 120$ K) [14], have presented some evidence for the appearance of tunneling in the reorientation of these B-H complexes in Si at $T < 70$ K. Also, recent path-integral calculations of hydrogen in crystalline silicon by Herrero show a change in the slope of the Arrhenius plot at ~ 80 K, signaling the onset of quantum tunneling of the impurity [15].

From a theoretical point of view, Flynn and Stoneham's theory (FST) of quantum diffusion of light interstitials gives a good description of tunneling processes in solids [3,11,16,17]. However, it is not clear the full applicability of this theory to defects in which the nonlinear coupling between the impurities and the lattice becomes relevant. In fact, for B-H complexes in silicon, Cheng and Stavola [12] obtained a reasonable value for the tunneling matrix element ($J = 56$ meV) by fitting the parameters in the FST to the hydrogen jump rate, but the Debye temperature ($\Theta_D = 187$ K) obtained in this fit is lower than the actual Debye temperature for silicon ($\Theta_D > 450$ K).

In this Letter, we present path-integral Monte Carlo (PIMC) simulations of the B-H and B-D complexes, which show the onset of thermally assisted tunneling for the hydrogen complex at $T \sim 60$ K. Both the anharmonicity of the interatomic potentials and the nonlinear coupling of the impurity to the lattice are included in the calculations. Our results indicate that the quantum fluctuations of the host atoms are basic to describe adequately the tunneling of the full complex.

We assume the validity of the Born-Oppenheimer approximation. The Si-Si interactions were described by the Stillinger-Weber (SW) potential [18]. The Si-B potential has been modeled by a SW-type potential, which was fitted to reproduce the vibrational frequencies of the boron local modes [8] and the B-Si distance [9] in boron-doped silicon. The Si-H interactions were modeled with an empirical three-body potential, previously used to study hydrogen in undoped silicon [19]. The B-H interactions have been described by a three-body potential developed to mimic as closely as possible the adiabatic energy surface calculated by Denteneer *et al.* for H^+ in boron-doped silicon [9]. With these interatomic potentials, the absolute minimum of the energy surface for H is found at a BM site, with an outward relaxation of the B and Si atoms of 0.17 and 0.30 Å, respectively. This translates into a Si-H (B-H) bond length of 1.48 Å (1.32 Å). The self-trapping energy (i.e., the raise in potential energy due to relaxation of the B and Si host atoms) is found to be 1.18 eV, a value much larger than that of 0.3 eV reported for hydrogen in Nb [17]. This energy is also considerably larger than the zero-point energy found for H at the BM site ($E_0 = 0.27$ eV). The calculated hydrogen frequency along the Si-B axis is 1947 cm^{-1}, to be compared with the experimental value [8] of 1903 cm^{-1}. The adiabatic barrier for hydrogen

motion, calculated by allowing full relaxation of the B and Si atoms, is 0.22 eV, and has its saddle-point at the site labeled C^* in Fig. 1. In this configuration, B is coordinated to four Si atoms and forms a B-H bond with a length of 1.2 Å.

Within the path-integral formalism, each quantum particle is represented as a cyclic chain of N beads coupled by harmonic springs, each chain configuration representing a quantum path [20]. The classical limit is obtained for $N = 1$. By taking sufficiently large values for N, the quantum mechanical partition function can be calculated with arbitrary accuracy. However, the calculation of reorientation rates of the complex cannot be done at present with the same rigor, but depends on a plausible assumption, formalized in the so-called quantum transition state theory (TST) [20]. This theory relates the jump rate k to the ratio, P_c, between the equilibrium probabilities for finding the center-of-gravity of the quantum paths (the so-called "centroid") [4,15,20] of the light-jumping impurity at the saddle point C^* and at the stable site BM. Namely:

$$k = \frac{1}{2}\,\overline{v}\,\frac{P_c}{L}\,, \tag{1}$$

where $\overline{v}$ is a weakly temperature-dependent factor taken to be the thermal velocity $\overline{v} = \sqrt{2/\pi\beta m}$, $\beta = (k_B T)^{-1}$, and L is the BM-C^* distance. The probability ratio P_c is given by [15,20]:

$$P_c = \exp\left(-\beta \int_{\mathbf{x}_{\mathrm{BM}}}^{\mathbf{x}_{C^*}} \mathbf{f}(\mathbf{x})\, d\mathbf{x}\right), \tag{2}$$

where $\mathbf{f}(\mathbf{x})$ is the mean force acting on the quantum impurity with its centroid fixed at $\mathbf{x}$. This force has been evaluated at 10 points along the path indicated by an arrow in Fig. 1. The integral in Eq. (2) is then calculated numerically, and gives the free energy barrier for the impurity jumps [20]. Within this approach, quantum effects such as phonon-assisted incoherent tunneling and the zero-point energy are included in the calculation of the activation energy. In our calculations, we use a $2 \times 2 \times 2$ supercell of the fcc diamond-type cell, where the B and ten Si nuclei nearest to the H impurity are treated either quantum-mechanically or classically (see below), while the other host atoms in the simulation supercell are kept fixed at their relaxed positions. See Refs. [15,19] for details on the Monte Carlo calculation.

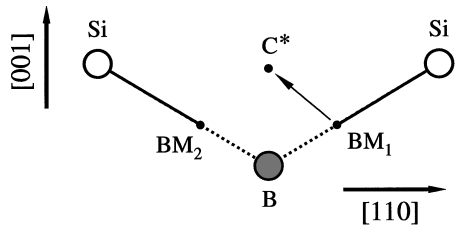

FIG. 1. Schematic representation of the B-H complex in silicon. BM_1 and BM_2 indicate two of the four stable sites for hydrogen around the B atom (dark circle). An arrow indicates the integration path from BM_1 to the saddle point C^* used in Eq. (2). The dotted lines indicate that H is weakly bound to B [10].

The jump rate of hydrogen and deuterium is shown in Fig. 2 vs the inverse temperature. The symbols are path-integral results: black squares for hydrogen, circles for deuterium, and triangles for hydrogen in a lattice of classical atoms. The dashed-dotted lines are linear fits to these path-integral results. The dashed line is a fit to the stress-induced dichroism results of Cheng and Stavola [12] for hydrogen, and the continuous line is an extrapolation of the internal friction results of Cannelli *et al.* [14]. The hydrogen jump rate derived from our simulations shows a break in the Arrhenius slope at ~ 60 K, which compares well with a crossover temperature of ~ 70 K found in Ref. [12]. For deuterium, no significant deviation from the high-temperature Arrhenius line is found down to 30 K, apart from the statistical noise of the results.

The parameters resulting from an Arrhenius fit for both the high- and low-temperature regimes are given in Table I. The prefactors derived from TST are larger than the experimental ones, as reflected in the shift of the calculated jump rates with respect to those derived from experiment (see Fig. 2). The high- and low-temperature activation energies are in reasonable agreement with the experimental values [12–14]. For hydrogen at low temperatures, we obtain an activation energy of 0.17 eV, somewhat lower than the high-temperature effective barrier of 0.20 eV. Both the low value of the pre-exponential factor at low temperatures, much smaller than a typical phonon frequency, and the value of the activation energy, lower than the high-temperature effective barrier, support the

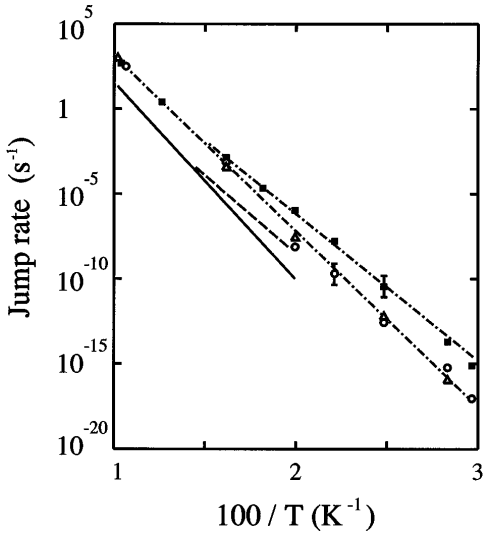

FIG. 2. Jump rate of hydrogen and deuterium. The symbols are PIMC results: black squares for hydrogen, circles for deuterium, and triangles for hydrogen with classical lattice atoms. The dash-dotted lines are linear fits to our simulation results for hydrogen. For comparison, the experimental results are dashed line for stress-induced dichroism results for hydrogen [12], and continuous line for the extrapolation of internal friction results [14]. Error bars give the statistical uncertainty of the simulation results.

TABLE I. Activation energy, prefactor, and crossover temperature T_C for the hydrogen jump rate, derived from our calculations and from experimental results 12,14.

Regime	E_A (eV)	Prefactor (s^{-1})	T_C (K)
high T, calc.	0.20	10^{13}	—
high T, expt.	0.223 ± 0.006	4×10^{12}	—
low T, calc.	0.17	5×10^{10}	~60
low T, expt.	0.176 ± 0.003	2×10^{9}	~70

interpretation of a transition from thermally activated quasiclassical jumping over the barrier to phonon-assisted tunneling [11]. The reduction of about 30 meV in the activation energy at temperatures below the crossover is found only in those simulations in which the four nuclei with largest participation in the reorientation of the defect complex (i.e., the three nuclei shown in Fig. 1 and the H impurity) are treated quantum mechanically. A quantum treatment of the proton and a classical one of the lattice gives no deviation of the Arrhenius law (triangles in Fig. 2) down to 25 K. Even if the quantum treatment is extended only to the B nucleus, no deviation from the Arrhenius law is found. This suggests a qualitative difference between H tunneling in metals and in doped silicon. Besides the classical thermal fluctuations, it is necessary to take into account quantum fluctuations of at least the B and two Si nuclei nearest to H, to obtain a coincidence geometry for tunneling. In the reported cases of H in metals, the lattice does not couple in this way to the hydrogen motion: thermal (classical) lattice fluctuations are sufficient to yield the coincidence geometry necessary for impurity tunneling [4,20].

The reverse isotope effect (D jumping faster than H) found from stress-induced dichroism in Ref. [12] is not reproduced by our PIMC simulations. In fcc metals, such as Pd, Cu, and Ni, it has been proposed [21] that a similar reverse isotope effect arises from the variation of the perpendicular zero-point motion along the diffusion path. However, with our potential model, no reverse isotope effect related to this zero-point motion is found. Also, hydrogen at the BM site induces a lattice relaxation lower than deuterium, because of its larger zero-point motion perpendicular to the B-Si axis [22]. Then, Cheng and Stavola's suggestion [12] that the reverse isotope effect is possibly due to the larger lattice relaxation in the case of H is not supported by our results. An explanation of this effect remains as a challenge, whose solution probably requires a treatment of the coupling between the nuclear dynamics and the electronic degrees of freedom.

The probability distribution for the nuclei, with the centroid of the impurity fixed at the saddle point, allows us to visualize the delocalization of the quantum particles in the coincidence geometry. The projection of this probability distribution along the [110] direction is shown in Fig. 3, for both hydrogen (a) and boron (b). At a temperature of 100 K, the hydrogen distribution shows a single maximum around the C^* site, which broadens with decreasing temperature. For temperatures below the crossover, it shows two well-defined peaks, corresponding to paths extending simultaneously into two neighboring potential wells, which indicates the appearance of quantum tunneling [15,20]. An important result is that the probability distribution for B goes through the same qualitative transition as hydrogen, from a single maximum at high temperatures to a bimodal distribution at temperatures lower than the crossover. The same occurs for the nearby Si atoms, although to a lesser extent (see later). This behavior provides a clear picture of the fact that the whole complex (H along with the lattice distortion around it) is undergoing quantum tunneling between two well-defined regions in the configuration space.

One can also monitor the transition between both regimes by looking at the evolution of the quantum delocalization (QD) of the nuclei with temperature. We call QD the mean-square radius of the path-coordinate with respect to the centroid of the path [19,20]. This is shown in Fig. 4 for (a) hydrogen and (b) boron, the nearest Si nuclei (shown in Fig. 1), and the bulk Si nuclei. Below the crossover temperature at ~60 K, a sharp increase in the QD is obtained for H, B, and the nearest Si nuclei. As expected, the delocalization of hydrogen is highly anisotropic and we find a nonspherical distribution with principal axes [110], [$1\bar{1}0$], and [001] (see Fig. 1). At 100 K, the QD along these axes is 0.026, 0.024, and 0.007 Å^2, respectively. At 30 K, we obtain the values 0.204, 0.027, and 0.014 Å^2. The sharp increase of the

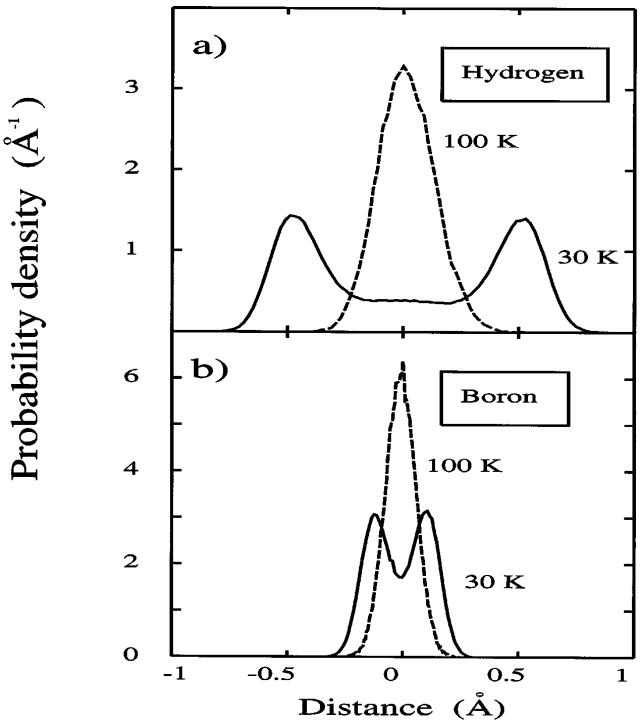

FIG. 3. Projection of the probability density for hydrogen (a) and boron (b) along the [110] direction (see Fig. 1), as obtained from PIMC simulations with the centroid of hydrogen fixed at the saddle point C^*.

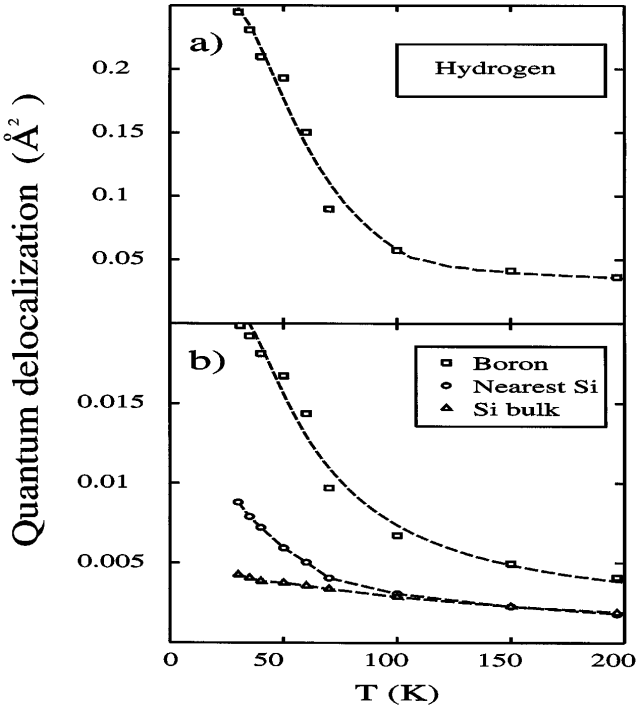

FIG. 4. Quantum delocalization of (a) H and (b) B, nearest Si nuclei and bulk Si, as obtained from the PIMC simulations with the centroid of H fixed at C^*. Dashed lines are guides to the eye.

QD along the [110] direction (BM_1-BM_2 direction) at temperatures below the crossover is in line with the transition found for the probability distribution of the paths, from a single maximum to a bimodal distribution. For the QD of the B nucleus, we find the same principal axes as for hydrogen, with values at 30 K of 0.015, 0.002, and 0.003 $Å^2$, respectively. Note that for both B and H nuclei, the largest QD corresponds to the [110] direction, reflecting the coupling between H and B in the tunneling process. For the nearest Si nuclei, the quantum delocalization is maximum along a direction close to the corresponding B-Si axis. The QD of the Si nuclei further than nearest neighbors of H, is not affected by the presence of hydrogen, and displays spherical symmetry.

In summary, by using PIMC simulations, with the limitations of the employed empirical potentials and the approximate treatment of the quantum dynamics, we have obtained jump rate constants for hydrogen and deuterium in boron-doped silicon, showing a break in the slope of the Arrhenius plot for hydrogen, which corresponds to a transition from quasiclassical thermally activated motion over the barrier to thermally assisted tunneling through the barrier at low temperatures. The bimodal probability distribution for both H and B nuclei in the coincidence geometry at temperatures lower than the crossover, and the sharp increase of the quantum delocalization of the H, B, and adjacent Si nuclei, indicate that the whole defect complex is undergoing quantum tunneling. The B-H complex in silicon is a prototype for other defects in solids with large self-trapping energy, for which one expects a behavior similar to that presented here.

This work was supported by CICYT (Spain) under Contract No. PB93-1254. One of us (J. C. N.) thanks the Ministerio de Educación y Cultura (Spain) for financial support.

[1] *Hydrogen in Semiconductors*, edited by J. I. Pankove and N. M. Johnson (Academic, New York, 1991).
[2] S. J. Pearton, J. W. Corbett, and M. Stavola, *Hydrogen in Crystalline Semiconductors* (Springer-Verlag, Berlin, 1992).
[3] C. G. Chen and H. K. Birnbaum, Phys. Status Solidi (a) **36**, 687 (1976).
[4] T. R. Mattsson, U. Engberg, and G. Wahnström, Phys. Rev. Lett. **71**, 2615 (1993).
[5] E. E. Haller, B. Joos, and L. M. Falicov, Phys. Rev. B **21**, 4729 (1980).
[6] K. Muro and A. J. Sievers, Phys. Rev. Lett. **57**, 897 (1986).
[7] G. G. DeLeo and W. B. Fowler, Phys. Rev. B **31**, 6861 (1985).
[8] C. P. Herrero, M. Stutzmann, and A. Breitschwerdt, Phys. Rev. B **43**, 1555 (1991).
[9] P. J. H. Denteneer, C. G. Van de Walle, and S. T. Pantelides, Phys. Rev. Lett. **62**, 1884 (1989); Phys. Rev. B **39**, 10 809 (1989).
[10] S. K. Estreicher, L. Throckmorton, and D. S. Marynick, Phys. Rev. B **39**, 13 241 (1989).
[11] A. M. Stoneham, Phys. Rev. Lett. **63**, 1027 (1989); M. Stavola, K. Bergman, S. J. Pearton, and J. Lopata, Phys. Rev. Lett. **63**, 1028 (1989).
[12] Y. M. Cheng and M. Stavola, Phys. Rev. Lett. **73**, 3419 (1994).
[13] M. Stavola, K. Bergman, S. J. Pearton, and J. Lopata, Phys. Rev. Lett. **61**, 2786 (1988).
[14] G. Cannelli, R. Cantelli, M. Capizzi, C. Coluzza, F. Cordero, A. Frova, and A. Lo Presti, Phys. Rev. B **44**, 11 486 (1991).
[15] C. P. Herrero, Phys. Rev. B **55**, 9235 (1997).
[16] C. P. Flynn and A. M. Stoneham, Phys. Rev. B **1**, 3966 (1970); A. M. Stoneham, J. Chem. Soc. Faraday Trans. **86**, 1215 (1990)
[17] H. R. Schober and A. M. Stoneham, Phys. Rev. Lett. **60**, 2307 (1988).
[18] F. H. Stillinger and T. A. Weber, Phys. Rev. B **31**, 5262 (1985).
[19] R. Ramírez and C. P. Herrero, Phys. Rev. Lett. **73**, 126 (1994); C. P. Herrero and R. Ramírez, Phys. Rev. B **51**, 16 761 (1995).
[20] M. J. Gillan, Phys. Rev. Lett. **58**, 563 (1987); Philos. Mag. A **58**, 257 (1988).
[21] S. Fujita and A. Garcia, J. Phys. Chem. Solids **52**, 351 (1991).
[22] C. P. Herrero and R. Ramírez, J. Phys.: Condens. Matter **8**, 8309 (1996).